

Rasterized Image Databases with LSH for Compression, Search and Duplicate Detection

Zoya Bylinskii
MIT CSAIL

Andrew Spielberg
MIT CSAIL

Maria Shugrina
MIT CSAIL

Wei Zhao
MIT CSAIL

ABSTRACT

TODO.

1. INTRODUCTION

Large collections of images are ubiquitous in the modern digital world. According to one 2014 Internet Trends report, more than 1.8 billion images are uploaded to the internet every day [7]. Our work is inspired by the intuition that there must be a lot of redundancy in large image collections, and that this redundancy could be exploited for more efficient storage and for applications such as duplicate detection.

We focus on image redundancy on the patch level, assuming that large collections of images must have many patches which are nearly the same. Our goal is to store a set of images as a database of similar patches, where similar patches may be shared between images, such that we minimize the storage space while maintaining certain *quality* of reconstructed images. In effect, this results in lossy compression. More concretely, we aim to choose a patch distance criterion, matching and reconstruction algorithms such that:

- the database size is smaller than if full images were stored
- the images can be reconstructed from the database in real time
- the reconstructed images fulfill certain quality requirements (See Sec. 6)

These conflicts introduce a number of tradeoffs, such as size of the database versus image quality. The goal of this paper is as much to produce a working system as to build up the analytical foundations that allow making these tradeoffs.

Section 2 covers some related work on image compression, raster databases, and patch-based computer vision applications. In section 3, we explain our method of “patchifying” images, storing them in a database, and reconstructing stored images. In section 4 we discuss how we accomplish

the fast retrieval of similar patches via locality-sensitive-hashing, which is crucial to the feasibility of our system. In section 5 we discuss other important database optimizations required for performance. In section 6, we provide the analytical groundwork for selecting optimal image patch sizes, distance thresholds, and quality metrics appropriate for evaluation. Finally, in section 7 we evaluate our full working system on real data, using the analytical tools developed from the previous section. In addition, in section 8, we briefly touch on applications that derive naturally from a patch database, including similar image retrieval and duplicate detection, as well as a fun photomosaic application. We conclude by discussing future extensions.

2. RELATED WORK

Lossless image compression techniques like *area coding* or *Huffman coding* give quality guarantees but do not always give sufficient savings (especially for unstructured images). Lossy image compression algorithms, on the other hand, are quite popular and used for most applications dealing with natural images, including storage in image datasets, and web transmission. Often, lossy compression depends on a quantization of image regions (e.g. all pixels in a block of the image receive the same color value). For instance, the *JPEG compression* standard partitions an image into non overlapping blocks and applies a discrete cosine transform to each block, quantizing the resulting coefficients. *Fractal compression* techniques [5] apply an iterative algorithm to images to encode images as fractal codes, capable of representing different parts of the images at different levels of detail. This algorithm makes use of self-similarities and is computationally expensive. However, due to fast decoding, it can be used for file downloads. All of these approaches, however, operate on a *within-image* basis, compressing an image using either a pre-specified dictionary (quantization) or using within-image similarity. Thus, these approaches provide constant savings for image databases of arbitrary sizes.

In the age of big data, when the amount of images in image collections grows at enormous rates, a compression scheme that scales with the database size seems most appropriate. Thus, we are interested in compression schemes that take into account *across-image* redundancy, not just *within-image* redundancy.

Some of our inspiration comes from *raster databases*, which encode images (often of geospatial data) as a set of smaller images/regions with locations in the original large image.

Such a set-up is convenient for transmission or data loading, as it is possible to load and process only parts of the image at a time. Geodatabases, such as *ArcGIS* are set-up this way [4].

We combine the idea of raster databases with the idea of image compression. Patch-based image representations are also used in computer vision for various tasks, including image matching [3], object recognition [11], and image processing [2]. Considering images as collections of patches allows for matching without rigid spatial constraints. In other words, such approaches can often find approximate image matches, such as different viewpoints of the same scene. Patch-based approaches have thus proven to be sufficient for scene recognition applications. We adapt a patch-based approach as well. Even very coarse-grained patches can provide sufficient visual information for scene recognition purposes. Thus, if we reconstruct images from approximately-similar coarse-grained patches, they will still provide sufficient input to scene classification algorithms, for instance.

3. APPROACH

To limit the complexity, we assume each image to be a square of m^2 pixels, and for all patches to be squares of the same size, n^2 . We formally describe our method in Sec. 3.1. To summarize, we first segment each image into patches and store them in the `patch_dict` table, a dictionary of patches. Only patches sufficiently different from all the other patches in `patch_dict` are subsequently added to the dictionary (see sec. 3.2). We describe our patch distance in sec. 3.3 and our implementation details in 3.4. Instead of storing each image explicitly, we store pointers to the patches approximating its original patches. Thus, during reconstruction, we simply stitch together the patches using pointers (sec. 3.5).

3.1 Overview

Our method is governed by the following parameters:

- m - The width and height of all images.
- n - The width and height of all patches¹.
- k - The number of images in our database.
- S - A distance function $S: \mathbb{I}_{n \times n} \times \mathbb{I}_{n \times n} \rightarrow \mathbb{N}$, where we define $\mathbb{I}_{n \times n}$ to be the space of all $n \times n$ image patches. Section 3.3 details distance measures. The distance function should be at least a pseudometric, so $S(P_1, P_2) = 0$ if and only if patches P_1 and P_2 are the same.
- T - A distance threshold, $T \in \mathbb{R}$; used as a maximum value we allow on S for patch mappings.

It is worth noting that we propose a *lossy* compression scheme ($T > 0$). For the remainder of the paper, when we use the term *images* we are referring to entire images from our database. When we use the term *image patches* we are referring to small $n \times n$ contiguous portions of images in our database. When we use the term *dictionary patches*, we are specifically referring to patches which we have chosen to store in our `patch_dict` and use for compression. Here we present an overview of our compression method; in subsequent subsections we delve into the details.

¹We assume that $m \bmod n$ is 0.

3.2 Algorithm

We begin our compression algorithm by seeding `patch_dict` with an initial set of dictionary patches. These patches are chosen from randomly selected $n \times n$ image patches from the entire image database (see sec. 6.2 for a discussion of this seeding strategy). During the image insertion step, we partition each of our images into $(\frac{m}{n})^2$ non-overlapping patches, with the intent of mapping each image patch P_j to a patch in `patch_dict`. Thus, rather than storing the original image patch for a given image, we simply store a pointer to a patch in `patch_dict`. The dictionary patch we choose is the one which is closest to the image patch according to some distance metric S , i.e. the patch P_{NN} in `patch_dict` such that $S(P_{NN}, P_j)$ is minimized. If $S(P_{NN}, P_j) > T$, we then store P_j as a new patch in `patch_dict` and add a pointer to this dictionary patch from the image (at the corresponding (x, y) location in the image). Algorithm 1 summarizes the image insertion procedure. Assuming that our patch dictionary is a good sample of the image patches in our image database, adding additional patches should be a relative rare procedure. We discuss how often these extra insertions are needed in sec. 7.1. Thus, the space savings come from only needing to store an effective pointer for each image patch, rather than the entire patch data. Note that the maximum threshold on the distance of image patches and dictionary patches guarantees that each compressed image is at most $\frac{mT}{n}$ away from its original counterpart in S .

Algorithm 1 Basic alg. to insert image I into database

```

1: Patches  $\leftarrow$  Patchify( $I, n$ )
2: for  $P_j$  in Patches do
3:    $P_{NN} \leftarrow \operatorname{argmin}_{P_i \in \text{patch\_dict}} \{S(P_i, P_j)\}$ 
4:   if  $S(P_{NN}, P_j) > T$  then
5:     insert  $P_j$  into patches
```

With a large table of patches, finding the closest patch can be computationally expensive. In order to speed up the search, we employ *locality sensitive hashing* (LSH). Although this softens the constraint that we always find the closest dictionary patch in `patch_dict` for each image patch, the closest patch is still found with very high probability, and in expectation the selected patch is still very similar. Section 5 details nearest-neighbor retrieval, and alg. 2 includes the algorithm updated to account for this optimization.

Algorithm 2 Modification of alg. 1 with approximation

```

1: Patches  $\leftarrow$  Patchify( $I, n$ )
2: for  $P_j$  in Patches do
3:    $SimPat \leftarrow \text{FindLikelySimilarPatches}(P_j, \text{patch\_dict})$ 
4:    $P_{ANN} \leftarrow \operatorname{argmin}_{P_i \in SimPat} \{S(P_i, P_j)\}$ 
5:   if  $S(P_{ANN}, P_j) > T$  then
6:     insert  $P_j$  into patches
```

We will define $M: \mathbb{I}_{n \times n} \rightarrow \mathbb{I}_{n \times n}$ to return the closest patch to P_j from the set of patches returned by `FindLikelySimilarPatches`. $M(P_j)$ is the approximate nearest neighbor to P_j . Thus, our compression problem can formally be stated as choosing a selection of image patch to dictionary patch mappings which minimizes the storage space usage of our

patch table, while constraining each image tile to be at most T away from its mapped patch. In other words,

$$\begin{aligned} & \underset{\text{patch_dict}, M}{\text{minimize}} \quad c(k, d, m, n) \\ & \text{subject to} \quad S(P_j, M(P_j)) \leq T, \quad j = 1, \dots, k \left(\frac{m}{n} \right)^2. \end{aligned}$$

where $c(\cdot, \cdot, \cdot, \cdot)$ is a cost function as defined in section 6.1.1, d is the number of patches in the dictionary (i.e. $d = |\text{patch_dict}|$), and k, m, n are as defined in 3.1.

Given our pointer representation, we are able to construct the compressed image quite efficiently. Given an image identifier, we iterate over all patch pointers stored with it, associated with each image location (x, y) .

3.3 Patch Distance Metric

There are many image similarity/distance metrics that have been developed for images (see [13] for a good survey), and our method is applicable to any metric that involves Euclidean distance over image features, its stacked color channel pixel values being the simplest case.

For the purpose of this project, we choose to use squared Euclidean distance over (CIE)LUV color space. Given two $n \times n$ patches P_i and P_j , we evaluate distance S per color channel u as follows:

$$S(P_i, P_j, u) = \frac{\|P_i(u) - P_j(u)\|^2}{n^2}$$

where $\|\cdot\|$ denotes standard Euclidean norm. We normalize by the dimensionality of the space to allow us to keep the distance threshold independent of the patch size. See section 6.3 for more details. A benefit of using a Euclidean distance metric is that it allows us to use LSH to retrieve patches that are likely to be similar.

3.4 Implementation

We used *postgresql* to construct our database, and used Java API to talk to the database from a custom executable. Locality sensitive hashing, image segmentation and reconstruction were all implemented in Java, and used to construct a hash table on patches in *postgresql*.

Our code is available at:

https://github.com/shumash/db_project

The $n \times n$ patches are stored as byte data in the `patch_dict` table. We store the patch pointers for each image in the `patch_pointers` table. The full schema looks as follows:

```
patch_dict(id int PRIMARY KEY,
           patch bytea);

images(id int PRIMARY KEY);

patch_pointers(img_id int REFERENCES images(id),
               patch_id int REFERENCES patch_dict(id),
               x int,
               y int);

patch_hashes(
    patch_id int PRIMARY KEY REFERENCES patch_dict(id),
    hash int);
```

where `patch_pointers.x` and `patch_pointers.y` refer to the left top corner location of each patch in the image.

A visualization of our schema is provided in fig. 1.

3.5 Image Reconstruction

To reconstruct an image, we simply follow the (logical) pointers in the corresponding `patch_pointers` database table entry to retrieve the patches from the `patch_dict` for each (x, y) location in the image:

Algorithm 3 Image reconstruction

```
1: PatchPointers  $\leftarrow$  getAllPatchPointers(patch_pointers)
2: PatchData  $\leftarrow$  getAllPatches(patch_dict, PatchPointers)
3: ResultImage  $\leftarrow$  []
4: for  $P_d$  in PatchData do
5:   ResultImage.set( $P_d.x, P_d.y, P_d.patch$ )
```

4. NEAR NEIGHBOR SEARCH

Fast retrieval of similar patches is crucial for making construction of a sizeable patch-based database feasible. This is essentially near-neighbor retrieval in relatively high dimensions $3 \cdot n^2$ (1875 for $n = 25$). Image retrieval has been addressed in a number of papers, including more complex feature representations [8]. Our problem is somewhat different from most of previous work in that the variability in small patches is much less than in regular-sized images, and semantic information is irrelevant, and vectors are much shorter than for regular-sized images. Thus, we focus on tuning a simple Locality-Sensitive Hashing variant for our particular application.

4.1 Locality-Sensitive Hashing

Locality-Sensitive Hashing (LSH) [1] is popular approach to approximate near-neighbor search in high dimensions. Because this approach is hashing-based, it is attractive for database applications, where entire lookup data structure cannot be stored in memory.

At a high-level, LSH applies a family of hash functions F_i :

Why we don't want many hash tables:

$$\begin{aligned} P[b(P_i) = b(P_j) | S(P_i, P_j) < T] &> P_1 \\ P[b(P_i) = b(P_j) | S(P_i, P_j) > cT] &< P_2 \end{aligned}$$

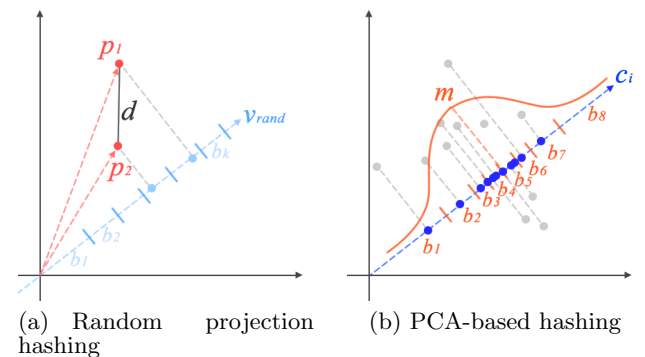


Figure 2: TODO.

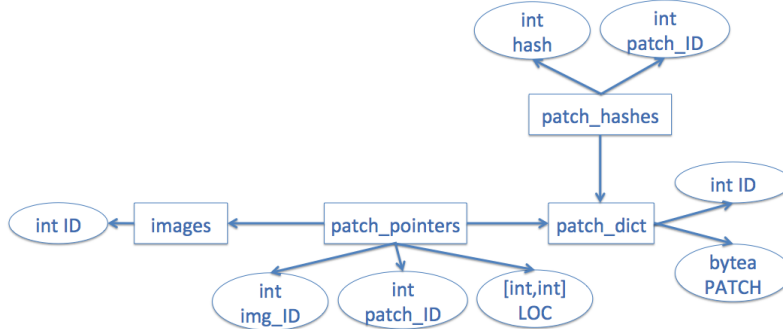


Figure 1: The proposed database schema.

4.2 Near-Neighbor Search with LSH

Using a single amplified hash function \mathcal{G} , finding all likely neighbors of a patch simply amounts to computing its hash value and taking all the patches that fall into the same hash bin. Moreformally, we can define the function in Alg. 2 as follows:

```

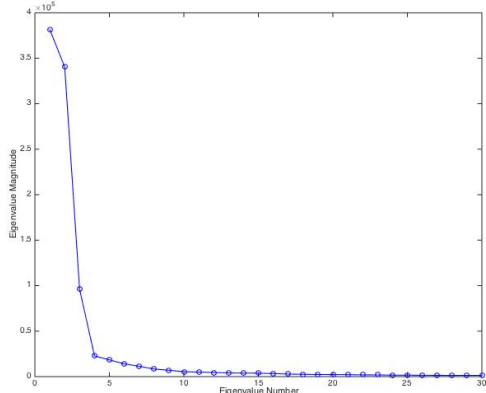
FindLikelySimilarPatches( $P_j$ ):
1:  $h \leftarrow \mathcal{G}(\text{ToVector}(P_j))$ 
2:  $\text{SimPat} \leftarrow \text{select patch from patch_dict where id in (select patch_id from patch_hashes where hash = h)}$ 

```

Of course, the quality of the result depends heavily on the properties of the hash function, which is something we discuss next.

4.3 Naive LSH

4.4 PCA-based LSH



We ran Principal Component Analysis (PCA) on 80K patch vectors sampled from 1000 images sampled uiniformly from all the categories in the SUN database [12].

4.5 Self-similarity Optimization

4.6 Color Uniformity

4.7 NN Results and Analysis

	time	#patches	#bins	FR	Stime	FPQ
Naive NN						
PCA NN	7h27min	3,309,583	2,751,235			
PCA + U NN						

Table 1: Results on 10,000 images samples from all the categories of the SUN database, where the rows are for naive projection hashing, PCA-based hashing and PCA-based hashing combine with uniform patch hashing.

We constructed 3 databases on the same set of 10,000 images sampled from all categories of the SUN database, with image size set to 500, and patch size set to 25, using the following hashing strategies for Near Neighbor(NN) search:

1. **Naive NN:** 10 random projection vectors sampled from unit Normal with uniform bin size (outliers truncated)
2. **PCA NN:** 10 first principla components as projection vectors with bin size adapted to the distribution of projections
3. **PCA + U NN:** nearly uniform patches are handled using a separate hash table, and non-uniform patches handled with PCA NN

To evaluate the results of this, we computed the following metrics.

PCA NN: Finished batch-upload of 10000 files in 26827397

5. DATABASE OPTIMIZATION

In this section we discuss additional optimizations to the database to make efficient construction of patch database feasible. Here and below I_{new} is an image about to be inserted into the database, and $P_1^n \dots P_j^n \dots$ are patches comprising it. To make large databases practical, our objective is to make the insertion process as fast as possible, given any of the Near Neighbor search methods described in Sec. 4.

5.1 Database Queries

Referring back to Alg. 2 and the definition of **FindLikelySimilarPatches** in Sec. 4.2, it is clear that to insert I_{new} , about $2\left(\frac{m}{n}\right)^2$ database queries are issued: $\left(\frac{m}{n}\right)^2$ for finding

near neighbors and at most $(\frac{m}{n})^2$ for inserting any patches without matches. This incurs a significant overhead, and we have modified our algorithm to make only at most 2 queries for every new image insertion. To accomplish this, we use batch query and insert, which result in 2 database queries, once to find all the likely similar patches, and once to insert new patches (See Alg. 4).

Algorithm 4 Optimization of alg. 2 for DB Queries

```

1: Patches  $\leftarrow$  Patchify(I, n)
2: Hashes  $\leftarrow$  []
3: for  $P_j$  in Patches do
4:    $P_j.h \leftarrow \mathcal{G}(\text{ToVector}(P_j))$ 
5:   add  $P_j.h$  to Hashes

6: NewPatchesToStore  $\leftarrow$  []
7: StoredPatches  $\leftarrow$  HashMap: hash  $\rightarrow$  [stored patches]
8: StoredPatches.FillFrom( select hash, patch from
   patch_dict, patch_hashes where hash in Hashes)
9: for  $P_j$  in Patches do
10:   SimPat  $\leftarrow$  StoredPatches[ $P_j.h$ ]
11:    $P_{ANN} \leftarrow \text{argmin}_{P_i \in \text{SimPat}} \{S(P_i, P_j)\}$ 
12:   if  $S(P_{ANN}, P_j) > T$  then
13:     NewPatchesToStore.Add( $P_j$ )
14:     StoredPatches[ $P_j.h$ ].Add( $P_j$ )
15: BatchInsert(NewPatchesToStore)

```

Please note that this hides some of the complexity, as we also need to keep track of pointer data, i.e. which stored patch ID each tile in the new image should point to. If *HashMap* contains newly processed patches that have not yet been inserted into the database, we need to make sure that in the end the pointers for the image contain the right database IDs.

5.2 Patch Buffer Pool

In order to further optimize performance, we implemented a *BufferPool* for patches with a least-recently-used (LRU) eviction policy. The LRU policy was picked based on the intuition that similar images are often processed together. This is particularly true if the database is constructed sequentially from a categorized database, such as SUN [12].

The function of the *BufferPool* is two-fold. In addition to minimizing database queries and random I/O for reading patches from disk, the *BufferPool* stores the hash value of each patch, as well as its vector form for faster computation of the distance S . These values are computed in a lazy fashion - only when requested. Given our unoptimized Java implementation of image vectorization and dot product, we found these measures to yield a non-negligible speed-up.

5.3 Exploiting Self-Similarity

TODO: shumash will rewrite this

*The idea of this algorithm is to do a local filtering among the patches of a single image before we query the database, such that the set of patches will only contain patches that are already greater than T distance away from each other. Let's call the filtered set the *unique patches*. Then we query the database to find the set of likely to be similar patches to each of the unique patches. Only if none of the likely-to-be similar patches in the database matches a patch from the unique patches, do we insert this patch.*

As discussed in [TODO], it is possible for similar patches to end up in different hash bins. Therefore, even if two patches p_1 and p_2 from a new image are similar to each other, they may return different bin numbers. To minimize the number of queries to the database, we have experimented with exploiting self-similar

In general, this is fine, but in the case of Naive Near Neighbor search, where bins can contain a lot of elements, each additional

6. PARAMETER ESTIMATION

A number of parameters can be tweaked to change the patch matching and storage, and different choices may be appropriate for different applications and performance requirements (both quantitative and qualitative). These parameters include the size of the input images, the size of the patches extracted, the sampling strategy used to seed the dictionary, the distance metric and thresholds used to compare patches, as well as the parameters required for indexing and retrieving patch matches (approximate nearest neighbors). Here we discuss some of the parameter choices made and the experiments that lead up to these choices. Other possible choices are discussed in Sec.8.4.

Our quantitative performance metrics involve examining how the patch dictionary size grows with the addition of new images to the database (the growth function and rate) and the compression ratio per image (viewed as a distribution over compression ratios and summarized as the average compression ratio). Qualitative evaluations involve determining whether a human can spot compression artifacts and how salient they are in the images. The authors of this paper manually examined images reconstructed from the dictionary patches. A crowdsourced evaluation strategy involving Amazon's Mechanical Turk may be appropriate for larger-scale studies, but was beyond the scope of this paper.

There will always be a trade-off between compression benefits (storage: patch dictionary size and speed: image reconstruction time) and reconstruction quality. For many computer vision tasks including scene recognition (and thus retrieval), imperfect reconstructions with artifacts may not be a problem as long as the overall scene structure does not change. For instance, [9] has shown that with images of pixel dimension 32x32, humans are already able to achieve over 80% scene and object recognition rate. See fig.3 for a demonstration of an image that has serious reconstruction artifacts, but when down sampled (to a thumbnail), they become insignificant, and thus do not necessarily impair visual recognition.

6.1 Patch Size

At larger patch granularities, each patch contains more image structure, and thus the probability that another patch contains the same or similar image content decreases with the number of pixels in a patch. At larger granularities it becomes increasingly harder to find matching patches in the patch dictionary, and the closest matching patches for textured regions might introduce artifacts (see fig.4). At the same time, patches that are too small do not offer as efficient a compression strategy. We must balance the costs of storing pointers to patches for each image in our database, as well as all the patches themselves, against the costs of storing the images in their original form. This calculation is investigated further below.

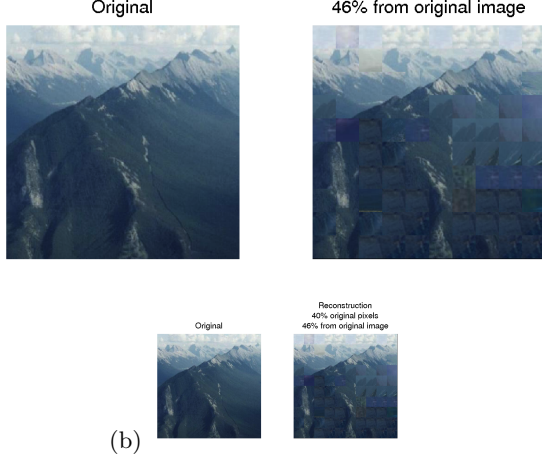


Figure 3: For demonstration purposes only, we choose a large patch size and low distance threshold. (a) Under these parameters, the original image is reconstructed to take up only 40% of its original size (in pixels). The 60% of the patches that have been replaced come either from the same image (46% of them), or from other images (the remaining 64%). (b) Notice that when the size of the image and its reconstruction are halved, the artifacts already become visually insignificant, and would not impair a scene recognition or search task.

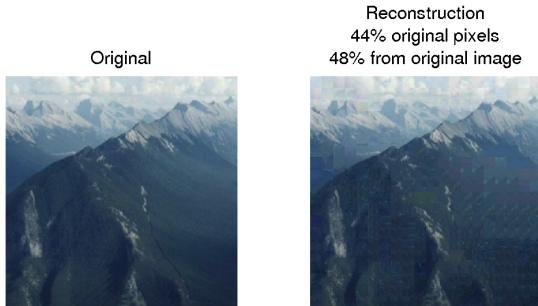


Figure 4: Compare this image reconstruction, computed with a dictionary of 25×25 pixel patches with the reconstruction in fig.3, computed with 50×50 patches. In both cases, a similar threshold is used (scaled to the patch size, as discussed in sec. 6.3) but the visual artifacts are less noticeable because smaller patches have less contained structure, and are more likely to be homogenous in appearance.

Optimal Cost vs. Number of Images and Patches in Database

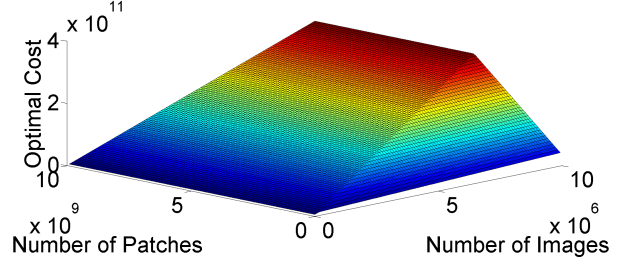


Figure 5: A graph demonstrating how c_{opt} changes with k and d for $m = 100$ and $n = 10$. Note the line of discontinuity where $d = 357.3k$ - this is the line where the costs of c and c' intersect.

6.1.1 Cost Evaluation

Assume, as before, that d is the number of patches in `patch_dict`. In practice, d is a function of the number of images added to the database as well as the distance function S and threshold T . We further assume that each pixel requires 3 bytes to store and that each pointer is 8 bytes (a standard integer for a 64-bit system). Then, with k images in the database, the full cost to store all the original images (no patch-based compression scheme) in our database is:

$$c'(k, m) = 3km^2 \quad (1)$$

In the case where we store pointers to patches, we have two tables: one table to store pointers to dictionary patches, and a second table to store the dictionary patches themselves. Under this ‘‘patch pointer’’ scheme, with k images and d patches, the cost c to store all the images in our database is:

$$c(k, d, m, n) = 8k \left(\frac{m}{n}\right)^2 + 3dn^2 \quad (2)$$

The first term is the cost of storing the pointer data, while the second term is the cost of storing the patches themselves. The 8 constant comes from the fact that we are dealing with very large image and patch tables ($> 2 \times 10^9$ patches), and thus a `bignum` type is required to store the patch references.

Given these two equations, for a fixed m and n , we can easily see that our compressive scheme becomes more space-efficient than storing the original images when:

$$d < \frac{m^2(3n^2 - 8)k}{3n^4} \quad (3)$$

As long as we choose a distance threshold such that new image patches get added at a rate that guarantees this inequality is satisfied, our compressive method of image storage will save space. Figure 5 shows an example of how the optimal storage cost changes with different patch and image counts, where the optimal cost is defined as $c_{opt} = \min(c, c')$; in other words, storing the images using the less expensive method. See fig. 5.

6.2 Sampling strategies

A patch dictionary can be built up incrementally, adding new patches as new images are added to the database. A po-

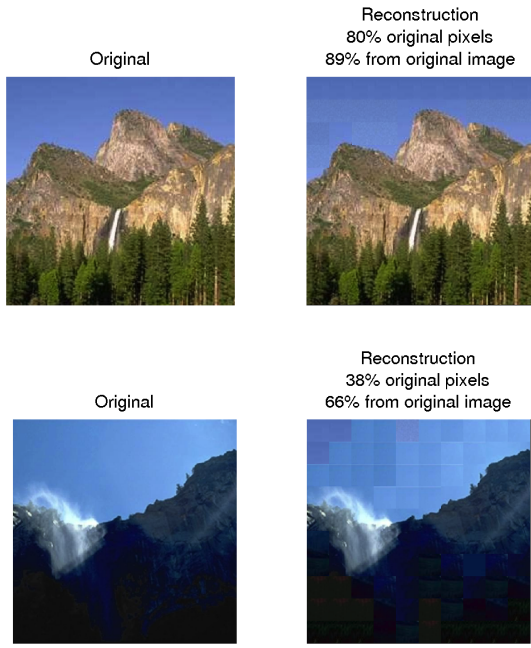


Figure 6: Example of a biased patch dictionary construction strategy, leading to non-uniformity in image reconstruction quality. Images added to the database earlier (top row) are better reconstructed (due to more patch samples in the database) than images added later (bottom row), constrained to be constructed out of patches added initially. The sky pixels in the image added later are borrowed from sky pixels of other images (44% of the pixels in this image come from other images, compared to only 11% in the image on the first row). Note: here we use a very high patch distance threshold and large patch size for demonstration purposes only, to emphasize the artifacts created.

tential problem with this approach is that image reconstruction quality will tend to decrease with the order in which images are added, such that images added to the database earlier will tend to have more patches that correspond to them (see Fig.6 for an example). A strategy with a more even distribution of reconstruction quality over images involves starting with a batch of images, and seeding the dictionary by randomly sampling patches from a set of images from the batch. This is the strategy we employ.

6.3 Distance Function

Many image (more specifically, patch) distance functions are possible, each with its own distinct set of parameters that can be tweaked for the required application. Because we are dealing with patches of a size specifically chosen to increase within-patch homogeneity, we do not consider cases of patches containing objects (the most we expect is an object boundary or simple texture), and thus do not need to consider complex image similarity/distance functions (involving SIFT, GIST, and other computer vision features). We can constrain ourselves to color distance, and split a patch P_i into 3 LUV color channels: $P_i(L)$, $P_i(U)$, $P_i(V)$.

Then we consider two patches P_i and P_j similar when, given $n \times n$ patches, all of the following are true:

$$\begin{aligned} \frac{1}{n^2} \|P_i(L) - P_j(L)\|^2 &< T_1 \\ \frac{1}{n^2} \|P_i(U) - P_j(U)\|^2 &< T_2 \\ \frac{1}{n^2} \|P_i(V) - P_j(V)\|^2 &< T_3 \end{aligned}$$

The $\frac{1}{n^2}$ term allows us to normalize for patch size, so that the threshold values chosen becomes independent of patch size. Here we constrain the average distance value of all the pixels in a patch to fit a threshold, whereas it is possible to have alternative constraints (where instead of the average, the maximal pixel difference or the variance of the pixel differences or some other measure over pixels in a patch, is compared to a threshold).

Note additionally that if instead we fix a single threshold for the sum of the Euclidean differences in the 3 color channels as in:

$$\frac{1}{n^2} [\|P_i(L) - P_j(L)\|^2 + \|P_i(U) - P_j(U)\|^2 + \|P_i(V) - P_j(V)\|^2] < T$$

then the similarity in one color channel may compensate for the difference in another, producing skewed results (see fig.7).

Multiple color channels are possible, but we choose to work in the (CIE)LUV color space, which is known to be more perceptually uniform than the standard RGB color space [6]. Additionally, our formulation makes it possible to impose separate distance thresholds on each of the color channels (T_1, T_2, T_3). However, for simplicity, we set $T_1 = T_2 = T_3 = T$, where the choice for the value of T is described next.

6.4 Distance Threshold

Choosing a threshold T requires weighing the quantitative benefits of compression with the qualitatively poorer image reconstructions. We ran a number of experiments, varying the threshold, and quantitatively and qualitatively examining the results. We rescale each color channel to be between 0 and 1, in order to choose a threshold T that is bounded by these values (and is independent of color representation). In fig. 8 we plot a few small experiments (with 200 images) for demonstrative purposes. The images were 500×500 pixels, and the patch size was 25×25 . We chose this patch size due to the discussion in 6.1. Below we consider a number of quantitative indicators for patch compression.

In the set of graphs in the first column of fig. 8, we plot in blue the dictionary size against the number of images added to the database. We compare this to the total number of patches that would have been stored if no compression scheme was utilized (red dotted line). We can see that for all choices of threshold, the size of the patch dictionary grows slower than the total number of patches that would need to be added if all images were stored along with their original patches. The gap between the blue and red dotted lines is a measure of the storage savings. As the threshold becomes more stringent, the blue line approaches the red dotted line. Note additionally that as the threshold becomes smaller, patches are more likely to be reused from the same image than from other images when compressing an image, because only patches from the same image will be similar enough to other patches from this image.

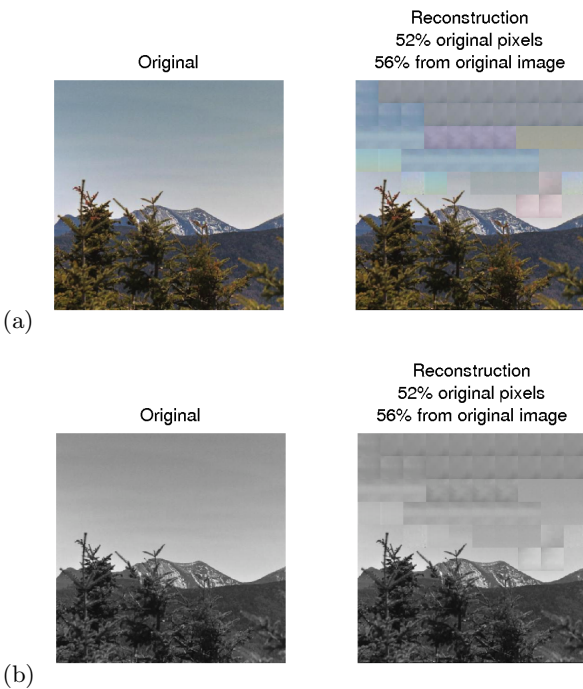


Figure 7: This is what happens when we do not separately constrain each of the color channels to match. We have patches that are (a) the wrong color and produce visible visual artifacts, while (b) matching in terms of general hue (average of the color channels). Again, the patch size and distance threshold were chosen to emphasize the artifacts.

The second column of fig. 8 contains histograms indicating how many images contributed different amounts of new patches to the patch dictionary. When the threshold is very small (as in the histogram in the last row) more of the images contribute most of their patches (380-400 new patches added to the patch dictionary per image). Note additionally that the small number of images that are contributing 0 new patches to the dictionary account for the 10% duplicates that are present in the SUN database (more about this in sec. 8.1).

The third column of fig. 8 contains an insertion history: for each image inserted into the database, we track how many of its patches were added to the patch dictionary. We can see that as the patch distance threshold decreases, most images contribute most of their patches. This provides similar information as the histogram (which is merely the cumulative), but allows us to monitor any temporal changes. The spikes to 0 in this graph are indicative of duplicate images, and are discussed further in sec. 8.1.

In the final column of fig. 8, we see a sample image reconstruction. We can see that the reconstruction quality increases, and visual artifacts decrease, as the distance threshold decreases (becomes more stringent). At some point in the middle, the reconstruction is already indistinguishable from the original, but with significant database compression benefits. Thus, for further analysis we consider the threshold $T = 8$ (recall that this is per color channel, and is independent of patch size).

7. EVALUATION AND DISCUSSION

In this section we evaluate the performance of the implementation of our method on a real collection of X images of Y size. [TODO](#)

7.1 Generalization across image categories and sizes

In the preceding sections, we determined that for an image sized 500×500 , a 25×25 patch size with a $T = 0.01$ patch distance threshold is appropriate since compression savings are properly balanced against artifacts introduced during image reconstruction. For further experiments, we scale down the image size to 100×100 and the patch size to 5×5 , accordingly, maintaining the patch:image size ratio. Note that the distance threshold still applies as it is independent of patch size. The reduction in image size allows us to consider larger experiments on databases of image thumbnails.

In fig. 9 we consider the growth of the patch dictionary as we add 2K images to our database. We add images from different categories, and observe a slight change in dictionary growth rate for every new category added. Although there is some variation across categories, the overall compression is 18.95% per image, demonstrating generalization across categories.

Not all image content is amenable to the same type of compression. For some types of images, particularly where there is a lot of spatial structure (e.g. indoors scenes with objects and parts), compression artifacts are much more noticeable and thus distance thresholds should be more stringent. An interesting extension that is beyond the scope of this paper would be to have a content-aware distance threshold (self-adjusting to content type such as indoor vs outdoor/natural).

For our database system, compression works for both indoor and outdoor images. In outdoor images, a lot of the compression savings come from accounting for the homogeneous sky patches (which may take up a large portion of the image). Although indoor images often contain many more objects and are more cluttered than outdoor images, they contain large homogenous regions corresponding to the walls and ceilings of rooms, which can surprisingly compress better than some outdoor images (walls may be more homogeneous than the sky). Thus, our compression approach generalizes to different types of scenes.

[If time allows, insert sample image reconstructions from different categories](#)

7.2 Quantitative

[TODO](#)

7.3 Qualitative

[TODO](#)

8. CONCLUSION

[Summarize paper contributions](#)

8.1 Applications

One of the appeals of this approximate patch-based approach is that it naturally lends itself to applications. In this section we describe methods to use our database for two applications - duplicate detection and similar image retrieval.

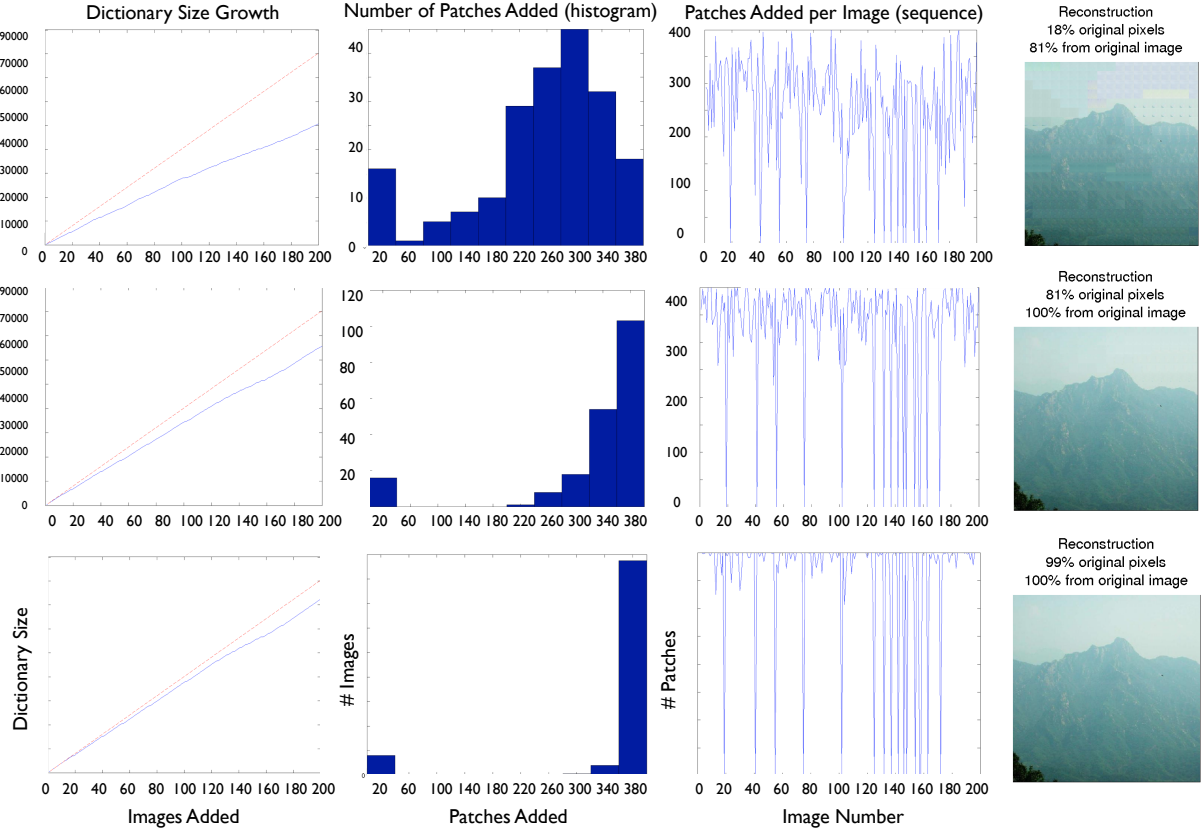


Figure 8: Quantitative and qualitative results obtained by varying the patch distance threshold, T , while extracting 400 patches from each image. In the first row, $T = 0.1$, the dictionary size is 50,822 patches, and the average compression per image is 36.73%. In the second row, $T = 0.01$, the dictionary size is 65,794 patches, and the average compression per image is 18.09%. In the third row, $T = 0.001$, the dictionary size is 72,445 patches, and the average compression per image is 9.80%.

8.2 Duplicate Detection

Encoding images as pointers to a collection of patches provides the ability to quickly spot images that contain large overlapping regions (composed of the same patches). In the extreme case, if multiple images point to the same set of patches, then we know these images are duplicates. Duplicates are a big problem in big computer vision datasets because they occur frequently and are hard to manually remove. They occur frequently (sometimes up to 10% of the time) because these datasets are automatically scraped from the internet, where the same image can occur under separate identifiers (on different websites, copied and uploaded by different users, etc.). The SUN database [12] used in this paper is no exception.

Duplicates are difficult to detect because not all duplicates are pixel-wise identical: the same image encoded using different standards or sized to different dimensions (even when resized to the same dimension later) will look almost identical to the human eye, but will contain different pixel values. Our patch distance metric is forgiving to perturbation at the pixel-level as long as the patch is overall similar to another patch (see sec.6.3). If multiple images map to the same set of patches that means that the corresponding patches in those images are within a distance threshold of each other (upper-bounded by $2T$). If multiple images map to all of the same patches, then we have good guarantees that the images are near-duplicates. Otherwise, the probability that every single patch matched would be low (i.e. low that two images are similar locally, for multiple local locations - as many locations as patches).

We can use these properties to spot duplicates in our database on-the-fly. For instance, when an image is added to the database, we can measure how many new patches the image contributed to the patch dictionary (because similar-enough patches could not be found), and how much of the image was mapped to pre-existing dictionary patches. When an image is reconstructed fully from the dictionary patches, and the patches it is reconstructed from all come from a single other image in the database, we know that the newly-added image is a duplicate. This is depicted in fig. 10.

By the same logic, similar images are those that overlap in terms of the patches they share in common. We can easily compare the two patch pointer vectors of two images to check their overlap. We can check if this overlap corresponds to patches clustered together in the images (for instance, when only some local region of the images matches, like when they share an object). We can thus discover images that have different degrees of overlap with other images.

8.3 Photomosaics

One interesting (and somewhat whimsical) application of our system is in the automated fabrication of photomosaics from images. A photomosaic² is an image which is created by partitioning a pre-existing 2-D piece of artwork into small, equally sized rectangles each of which is then replaced with a small image which approximates the original color and texture of the rectangle, keeping the overall artwork recognizable. Thus, the final result is an image composed of hundreds of smaller images.

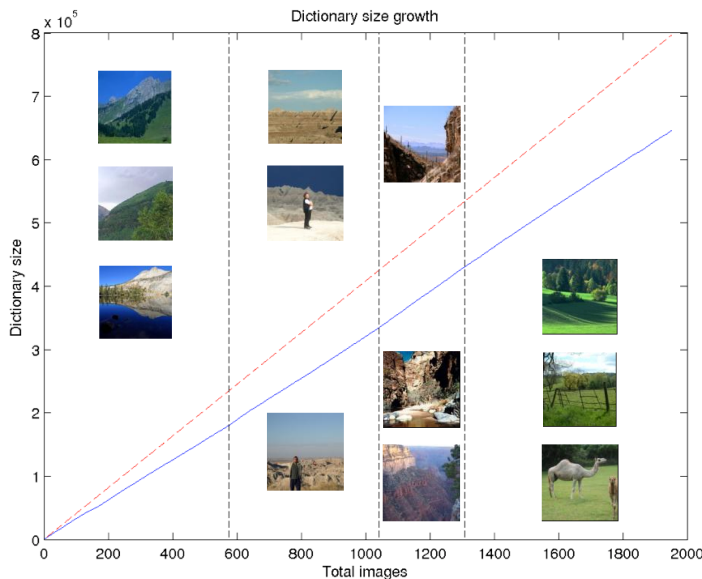


Figure 9: A patch dictionary constructed from 5×5 patches from 100×100 images, with a $T = 0.01$ patch distance threshold, obtains an average compression of 18.95% per image. The average number of new patches added per image is 330.70 with a total dictionary size of 645,534 patches representing 1952 images. The black dotted vertical lines mark the addition of new image categories, (left to right) mountain (with dictionary growth rate 312.96, equivalent to compression of 21.76% per image), badlands (growth rate 330.50, compression 17.38%), canyon (growth rate: 360.61, compression 9.85%), and pasture (growth rate: 334.11, 16.47%). A few image samples from the 4 categories are included. Note that for this growth rate, storing image patches will always take less space than storing the entire image, since $c < c'$.

²See, for example, http://en.wikipedia.org/wiki/Photographic_mosaic.

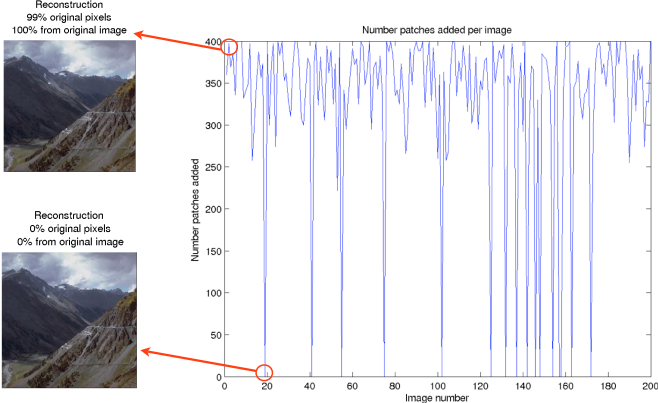


Figure 10: This is an example of the first 200 consecutive insertion queries to an empty database: for each image inserted, we can measure how many new patches were added to the patch dictionary (out of 400 patches in the image). When we see that this number spikes down to 0 we know that the image has been fully reconstructed from patches from other images. We can check if all those patches came from a single other image. If that is the case, we know we have a duplicate or near-duplicate image.

Our system can be directly applied to the synthesis of such images, with a few very small modifications. First, instead of determining which patches to store based on our previous dictionary and image collection, we a priori store a selected input image set as our patch dictionary, but scaled to "patch size." For demonstration purposes, we created our patch dictionary by scaling down and storing the entire SUN database. In order to create the photomosaic, we first choose and store a target image we would like to transform. In storing the image, we, as usual split the image into patches, and for each patch perform a nearest neighbor search. However, in this case, if no patch already exists in the hashed bin, we expand our nearest neighbor search to more bins until we find a bin with at least one patch, and choose the most similar one. During this step, we *never* store patches; we always map the patch to one already in the dictionary. The mapping output by this process results in a photomosaic.

We demonstrate this process on a 1600x1200 image of the Stata Center at MIT, using 25x25 rectangular patches. We show the original image and reconstruction in figure 11.

8.4 Future Extensions

In this paper we considered a simple implementation of a patch-based image database compression scheme, where the images and patches were square and of fixed sizes. Patches were sampled in a regular, non-overlapping grid from each image. Alternative approaches include more flexible, context-aware, patch-sampling techniques. For instance, the patch granularity for sampling large homogenous sky and field regions may be different from the one used for sampling highly-textured regions like objects and structures (trees, buildings, people, etc.). Similarly, patches that do not cross object boundaries are likely to lead to less artifacts in future

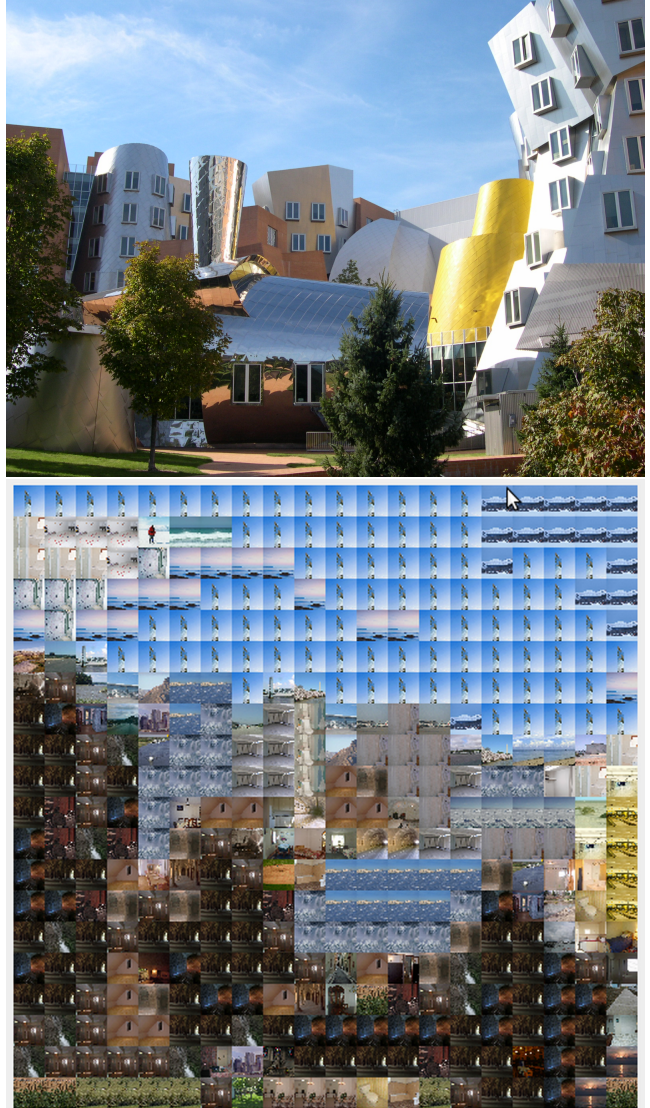


Figure 11: A sample photomosaic automatically generated by our system, with only a few small modifications as described in 8.3.

reconstructions. For this, approaches like Selective Search [10] that localize image regions likely to contain objects, may prove promising for sampling patches.

If patches were different sizes, then one of a number of extensions to the system would be required - for instance, (1) a patch transformation scheme, or (2) a hierarchical patch dictionary. A patch transformation scheme would permit each patch to be transformed (in a simple way - e.g. via rescaling) to match another patch with the same appearance but different (scale) parameters. For instance, a small patch in one image may be sufficient to account for a much larger part of another image, and rather than storing many separate patches of different sizes, we would benefit from quickly applying transformations to existing dictionary patches. To implement this system would require storing, for each image location, not only a pointer to a patch in the patch dictionary but also a transformation (e.g. a set of scaling parameters). Naturally, the cost function (to weigh the benefits of such a scheme vs storing the original images or even equally-sized patches) would need to take into account (a) the extra parameters stored along with each image location, and (b) the reconstruction time overhead for patch transformation. With large enough datasets, this approach may be effective at eliminating redundancy.

Another approach, building hierarchical patch dictionaries, may speed up the patchifying and subsequent reconstruction of an image, by offering a top-down approach. If larger patches match, there is no need to parse the image at a finer-grained scale. Only if large patches do not properly account for the structure in an image, would it be necessary to go to a finer-grained patch size. Note that small patches could be composed into larger patches, via a hierarchy, so that if large-patch matches are not found, descending down the patch hierarchy of the best-matching large patches would make it possible to find a match at a lower granularity. This scheme would be less flexible than the patch transformation scheme, but may prove to be more efficient.

9. REFERENCES

- [1] A. Andoni and P. Indyk. Near-optimal hashing algorithms for approximate nearest neighbor in high dimensions. *Commun. ACM*, 51(1):117–122, Jan. 2008.
- [2] C. Barnes, E. Shechtman, A. Finkelstein, and D. B. Goldman. PatchMatch: A randomized correspondence algorithm for structural image editing. *ACM Transactions on Graphics (Proc. SIGGRAPH)*, 28(3), Aug. 2009.
- [3] M. Brown. Multi-image matching using multi-scale oriented patches. In *CVPR*, pages 510–517, 2005.
- [4] E. S. R. Institute. Arcgis desktop: Release 10, 2011.
- [5] A. E. Jacquin. Image coding based on a fractal theory of iterated contractive image transformations. *IEEE Transactions on Image Processing*, 1992.
- [6] H. Kekre and V. K. Banura. Performance comparison of image retrieval using kfcp with assorted pixel window sizes in rgb and luv color spaces 1. 2012.
- [7] M. Meeker. Internet trends 2014 - code conference, 2014.
- [8] F. Perronnin, Y. Liu, J. Sánchez, and H. Poirier. Large-scale image retrieval with compressed fisher vectors. In *Computer Vision and Pattern Recognition (CVPR), 2010 IEEE Conference on*, pages 3384–3391. IEEE, 2010.

- [9] A. Torralba, R. Fergus, and W. T. Freeman. 80 million tiny images: a large database for non-parametric object and scene recognition. *IEEE PAMI*, 30(11):1958–1970, November 2008.
- [10] J. R. R. Uijlings, K. E. A. van de Sande, T. Gevers, and A. W. M. Smeulders. Selective search for object recognition. *International Journal of Computer Vision*, 104(2):154–171, 2013.
- [11] A. Vashist, Z. Zhao, A. Elgammal, I. Muchnik, and C. Kulikowski. Discriminative Patch Selection using Combinatorial and Statistical Models for Patch-Based Object Recognition. In *Proceedings of the 2006 Conference on Computer Vision and Pattern Recognition Workshop*. IEEE Computer Society Washington, DC, USA, 2006.
- [12] J. Xiao, J. Hays, K. Ehinger, A. Oliva, and A. Torralba. Sun database: Large-scale scene recognition from abbey to zoo. *IEEE Conference on Computer Vision and Pattern Recognition*, 2010.
- [13] M. Yasmin, M. Sharif, and S. Mohsin. Use of low level features for content based image retrieval: Survey. *Research Journal of Recent Sciences*, 2277:2502, 2013.